nologies. CNNs are also suitable to be involved in DNA microarray processing from different points of view. In fact, the analysis to be performed faces with a matrix of DNA sites, both in the case of fluorescence images, and in all the other cases in which hybridization results are read out on-site using electrical, optical or chemical methods. Rather, in the latter cases CNN technology gives the best way to analyze analog information in real time, as soon as the hybridization results are obtained from the chemical process, so avoiding any data conversion. The possibility to build CNN chips directly connected with a DNA microarray opens the way to powerful systems-on-a-chip for real time diagnosis.

ACKNOWLEDGMENT

The authors would like to thank Prof. L. O. Chua and Prof. T. Roska for their scientific interest in this activity and to Prof. G. Ferla from STMicroelectronics for supporting this R&D activity in the framework of cooperation between the University of Catania and STMicroelectronics. Moreover the authors are grateful to M. Purrello, Professor of Genetics at the University of Catania, for his helpful suggestions and encouragement.

REFERENCES

[1] "Genetics Supplement," *Nature*, vol. 21, Jan. 1999.
[2] M. Roos, "Medical electronics," *IEEE Spectrum*, Jan. 2000.
[3] L. O. Chua and T. Roska, "The CNN paradigm," *IEEE Trans. Circuits Syst. I*, vol. 40, pp. 147–156, Mar. 1993.
[4] W. W. Evans and M. V. Relling, "Pharmacogenomics Translating functional genomics into rational therapeutics," *Science*, vol. 286, no. 5439, pp. 487–491, 1999.
[5] The Human Genome Program. [Online]. Available: http://www.ornl.gov/TechResources/Human_Genome/home.html.
[6] J. L. DeRisi, V. R. Iyer, and P. O. Brown, "Exploring the metabolic and genetic control of gene expression on a genomic scale," *Science*, vol. 278, no. 5338, pp. 680–686, 1997.
[7] GeneChip Probe Array Technology. [Online]. Available: http://www.affymetrix.com/technology/tech_probe.html.
[8] S. Chan, P. M. Fauchet, Y. Li, L. J. Rothberg, and B. L. Miller, "Porous silicon microcavities for biosensing applications," *Phys. Stat. Sol. (a)*, vol. 182, pp. 541–546, 2000.
[9] D. Porath, A. Berzyadin, S. De Vries, and C. Dekker, "Direct measurement of electrical transport through DNA molecules," *Nature*, vol. 403, pp. 635–638, 2000.
[10] L. O. Chua and L. Yang, "Cellular neural networks: Theory," *IEEE Trans. Circuits Syst.*, vol. 35, pp. 1257–1272, Oct. 1988.
[11] ——, "Cellular neural networks: Applications," *IEEE Trans. Circuits Syst.*, vol. 35, no. 10, pp. 1273–1290, Oct. 1988.
[12] A. Rodriguez-Vazquez and T. Roska, "Review of CMOS implementations of the CNN universal machine-type visual microprocessors," in *Proc. ISCAS'00*, Geneva, May 28–31, 2000.
[13] T. Roska, L. Kek, L. Nemes, A. Zarandy, and P. Szolgay, "CSL CNN Software Library (Templates and Algorithms) Vers. 7.3,", Budapest, Hungary, Aug. 1999.
[14] Aladdin V.1.3, "Algorithm Design Using High Level Description and Visual Input Via the Alpha Language and Compiler: User's Guide," Analogic Computers Ltd., Budapest, Hungary, 2000.
[15] Aladdin V.1.3, "Extended Analogic Macro Code (AMC) and Interpreter: Reference Manual," Analogic Computers Ltd., Budapest, Hungary, 2000.
[16] I. Szatmari, A. Zarandy, P. Földesy, and L. Kek, "An analogic CNN engine board with the 64 × 64 analog I/O CNN-UM chip," in *Proc. ISCAS'00*, Geneva, Switzerland, May 28–31, 2000, pp. II-124–II-127.
[17] DICTAM Project Home Page. [Online]. Available: http://www.imse.cnm.es/~dictam/.

Complex Dynamic Phenomena in Space-Invariant Cellular Neural Networks

M. Biey, M. Gilli, and P. Checco

***Abstract*—It is shown that first-order autonomous space-invariant cellular neural networks (CNNs) may exhibit a complex dynamic behavior (i.e., equilibrium point and limit cycle bifurcation, strange and chaotic attractors). The most significant limit cycle bifurcation processes, leading to chaos, are investigated through the computation of the corresponding Floquet's multipliers and Lyapunov exponents. It is worth noting that most practical CNN implementations exploit first-order cells and space-invariant templates: so far no example of complex dynamics has been shown in first-order autonomous space-invariant CNNs.**

***Index Terms*—Cellular neural networks, chaotic dynamics, complex dynamics.**

I. INTRODUCTION

Cellular neural networks (CNNs) are analog dynamic processors, that have found several applications for the solution of complex computational problems [1]–[5]. A CNN can be described as a two- or three-dimensional array of identical nonlinear dynamical systems (called cells), that are locally interconnected. This property has allowed the realization of several high-speed VLSI chips [6], [7]. In most applications the connections are specified through space-invariant templates (that consist of small sets of parameters identical for all the cells.)

The mathematical model of a CNN consists in a large set of coupled nonlinear differential equations, that have been mainly studied through extensive computer simulations.

For what concerns the dynamic behavior, CNNs can be divided in two classes: stable CNNs, with the property that each trajectory (with the exception of a set of measure zero) converges toward an equilibrium point; unstable CNNs, that exhibit at least one attractor, that is not a stable equilibrium point. The stability results are summarized in [8], whereas some examples of CNNs presenting periodic limit cycles are shown in [9], [10].

Complex dynamics in CNNs (i.e., networks presenting nonperiodic, possibly strange, attractors) have been so far observed only in four cases: a) nonautonomous networks composed by two cells [11]; b) autonomous CNNs described by space-variant templates and composed by three cells [12]; c) delayed CNNs [13]; d) state-controlled CNNs [14]. So far, no example of complex dynamics has been shown in first-order autonomous CNNs, described by space invariant templates.

The importance of investigating the complex dynamic behavior of first-order autonomous space-invariant CNNs relies on the fact that such a model is exploited by most VLSI implementations [6]. The identification of chaotic dynamics in these networks might open the possibility of developing, on the existing CNN chips, innovative chaos-based applications.

In this brief we firstly consider the original Chua–Yang model and show that for a class of two-dimensional opposite-sign templates, complex dynamic occurs. Starting from a stable CNN, we investigate the

Manuscript received April 12, 2001; revised October 15, 2001. This work was supported in part by Ministero dell'Istruzione, dell'Università e della Ricerca, under the National Research Plan PRIN 2001 and in part by Consiglio Nazionale delle Ricerche (CNR), under Contract CNRG000D51. This paper was recommended by Associate Editor P. Szolgay.

The authors are with the Department of Electronics, Politecnico di Torino, Turin, Italy (e-mail: gilli@polito.it).

Publisher Item Identifier S 1057-7122(02)02270-5.

equilibrium point bifurcation, leading to periodic attractors. Then we study the limit cycle bifurcation route to chaos, through the computation of the corresponding Floquet's multipliers (FMs) and Lyapunov exponents. Then we consider the CNN modified model described in [15], that is more suitable for VLSI implementation: we show that also this model exhibits complex dynamic phenomena.

II. Space-Invariant CNNs

We consider CNNs composed by $N \times M$ cells arranged on a regular grid. We denote the position of a cell with two indexes $(k,\ l)$ with the assumption that cell (1, 1) is located in the upper left corner and cell $(N,\ M)$ is located in the lower right corner.

The network dynamics is described by the following normalized state equations [3]

$$\dot{x}_{kl} = -x_{kl} + \sum_{|n|\le r,\,|m|\le r} A_{n\,m}\, y_{k+n,\,l+m} + \sum_{|n|\le r,\,|m|\le r} B_{n\,m}\, u_{k+n,\,l+m} + I \quad (1)$$

where x_{kl} and u_{kl} represent the state-voltage and the input voltage of cell $(k,\ l)$; y_{kl} is the output voltage; r denotes the neighborhood of interaction of each cell; A_{nm} and B_{nm} are the elements of the linear templates $\boldsymbol{A}$ and $\boldsymbol{B}$, that are assumed to be space-invariant, and I is the bias term.

In the original Chua–Yang model [1] it is assumed that the output voltage y_{kl} depends on the state-voltage x_{kl} through the following piecewise-linear function $f_Y(\cdot)$:

$$y_{kl} = f_Y(x_{kl}) = \tfrac{1}{2}\left(|x_{kl}+1| - |x_{kl}-1|\right). \quad (2)$$

The function above is Lipschitz, but does not admit of a continuous derivative at $x_{kl} = \pm 1$. Such a critical behavior can cause some numerical problems to the limit cycle bifurcation analysis, that in most cases requires to evaluate the global derivative of function $f_Y(\cdot)$ [17]. For this reason, we assume that the relationship between the output and the state voltage is defined through the following function $f_\varepsilon(\cdot)$ that depends on the parameter ε

$$f_\varepsilon(x) = \begin{cases} -1, & x < -(1+\varepsilon) \\ \dfrac{1}{4\varepsilon}[x^2 + 2(1+\varepsilon)x + (1-\varepsilon)^2], & |x+1| < \varepsilon \\ x, & |x| < (1-\varepsilon) \\ -\dfrac{1}{4\varepsilon}[x^2 - 2(1+\varepsilon)x + (1-\varepsilon)^2,] & |x-1| < \varepsilon \\ 1, & x > 1+\varepsilon. \end{cases} \quad (3)$$

It is easily seen that f_ε is Lipschitz and also admits of a continuous first-order derivative [i.e., it belongs to the class $C^1(-\infty,\ \infty)$]. Function f_ε differs from f_Y only in the sub-intervals $]-(1+\varepsilon),\ -(1-\varepsilon)[$ and $](1-\varepsilon),\ (1+\varepsilon)[$. In addition we note that: 1) For small values of the parameter ε the two functions f_ε and f_Y cannot be distinguished (see Fig. 1); 2) In real circuits, piecewise-linear characteristics cannot be exactly realized; therefore f_ε represents the best approximation of the actual output functions implemented in those VLSI realization, that adopt the original Chua–Yang model [7]; 3) extensive simulations have shown that for $\varepsilon \le 0.15$, the qualitative dynamics of the two models (i.e., using f_Y or f_ε) is identical.

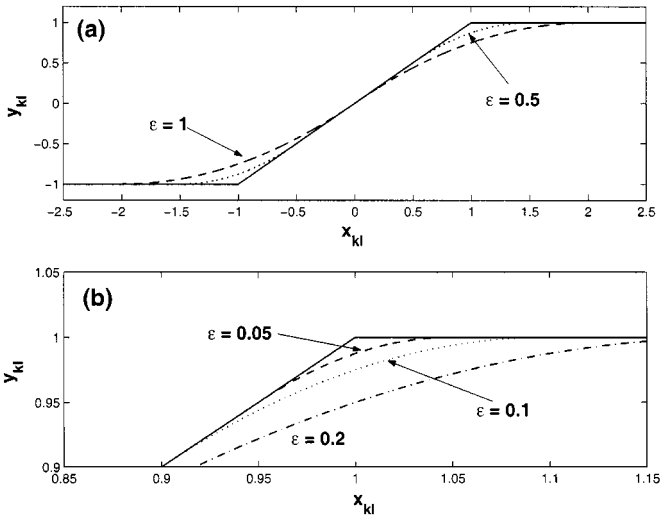

Fig. 1. Comparison between the smooth function $f_\varepsilon(\cdot)$ and the piecewise-linear function $f_Y(\cdot)$. (a) $\varepsilon = 1,\ 0.5$. (b) zoom in the neighborhood of $x_{kl} = 1$, for $\varepsilon = 0.2,\ 0.1,\ 0.05$.

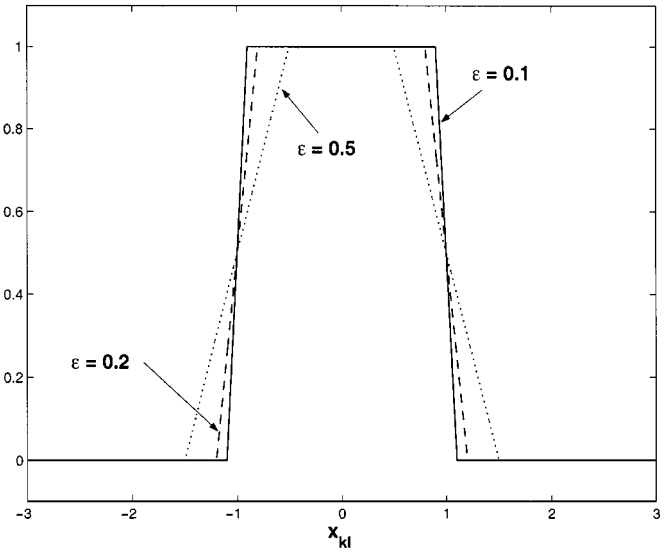

Fig. 2. First-order derivative of the smooth function $f_\varepsilon(\cdot)$ for $\varepsilon = 0.5,\ 0.2,\ 0.1$. Note that it is continuous at $x_{kl} = \pm 1$.

The analytical expression of the continuous first-order derivative of $f_\varepsilon(x)$ is reported below; the graphic is shown in Fig. 2

$$f'_\varepsilon(x) = \begin{cases} 0, & x < -(1+\varepsilon) \\ \dfrac{1}{2\varepsilon}\,[x + (1+\varepsilon)], & |x+1| < \varepsilon \\ 1, & |x| < 1-\varepsilon \\ -\dfrac{1}{2\varepsilon}\,[x - (1+\varepsilon)], & |x-1| < \varepsilon \\ 0, & x > 1+\varepsilon. \end{cases} \quad (4)$$

We will exploit the modified model introduced above for studying and detecting the most significant bifurcation processes occurring in space-invariant CNNs with first-order cells. Then we will show that similar phenomena can also be observed if different models, more suitable for VLSI implementations, are used (see [15]).

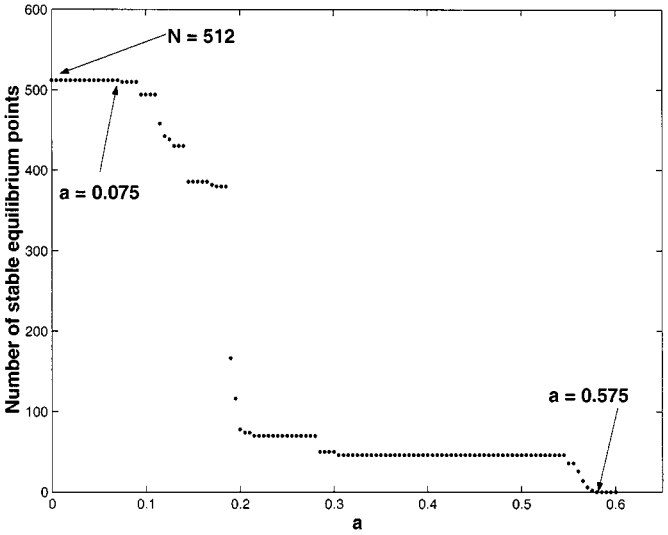

Fig. 3. Number of stable equilibrium points as a function of a.

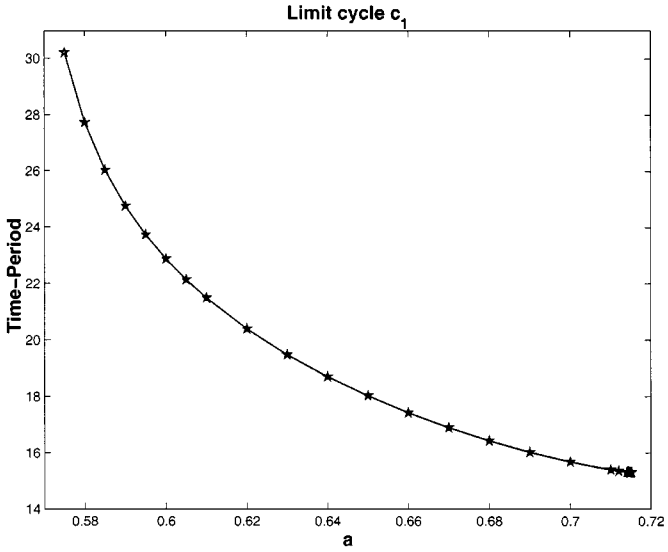

Fig. 4. Limit cycle c_1: time period versus a.

III. Complex Dynamics

We consider an autonomous CNN composed by 3×3 cells, with zero boundary conditions and zero input voltages, and described by the following opposite-sign $\boldsymbol{A}$ template

$$\boldsymbol{A} = \begin{bmatrix} a & a & a \\ -a & b & a \\ -a & a & -a \end{bmatrix} \quad \text{with} \quad b > 1;\ a > 0. \tag{5}$$

We assume that the output function is modeled by (3) with $\varepsilon = 0.1$.

We note that for such a CNN, the system of equations (1) is invariant under the following coordinate transformation:

$$\mathcal{T} \rightarrow \begin{cases} z_{11} = -x_{33} & z_{12} = x_{32} & z_{13} = -x_{31} \\ z_{21} = -x_{23} & z_{22} = x_{22} & z_{23} = -x_{21} \\ z_{31} = -x_{13} & z_{32} = x_{12} & z_{33} = -x_{11}. \end{cases} \tag{6}$$

In addition the system of equations (1) is odd; hence it is also invariant under the transformation

$$\mathcal{O} \rightarrow z_{ij} = -x_{ij}. \tag{7}$$

It turns out that if the CNN presents an invariant limit set l (i.e., an equilibrium point, a limit cycle, a chaotic attractor), then it should also exhibit: a) the limit set obtained by applying to l the coordinate transformation $\mathcal{T}(l)$; b) the two limit sets symmetric to l and $\mathcal{T}(l)$ with respect to the origin, i.e., $\mathcal{O}(l)$ and $\mathcal{O}[\mathcal{T}(l)]$.

The above class of templates (5) exhibits the following property: by increasing a all the stable equilibrium points disappear; since each trajectory is bounded, the network should present at least one attractor, that is not an equilibrium point (i.e., either a periodic or a nonperiodic attractor).

We assume $b = 1.6 > 1$ and investigate the dynamics of the network and the related bifurcation processes, that can be observed by varying the parameter a.

For $a = 0$ the cells are not coupled and each of them presents two stable equilibrium points, with output voltage $y_{kl} = \pm 1$, respectively. The whole network exhibits 2^9 stable equilibrium points. We have verified that, by increasing a, all the stable equilibrium points undergo a saddle-node bifurcation. The results are summarized in Fig. 3, that reports the number of stable equilibrium points as a function of the template parameter a: it is seen that the first saddle-node bifurcation occurs for $a = 0.075$, whereas the last one occurs for $a = 0.575$. For $a \geq 0.575$ the network does not present any stable equilibria; the simulations show that a stable limit cycle emerges (it will be denoted as c_1). Such a cycle probably originates through an heteroclinic bifurcation, since its period increases and tends to a vertical asymptote, as a approaches the value 0.575 (see Fig. 4).

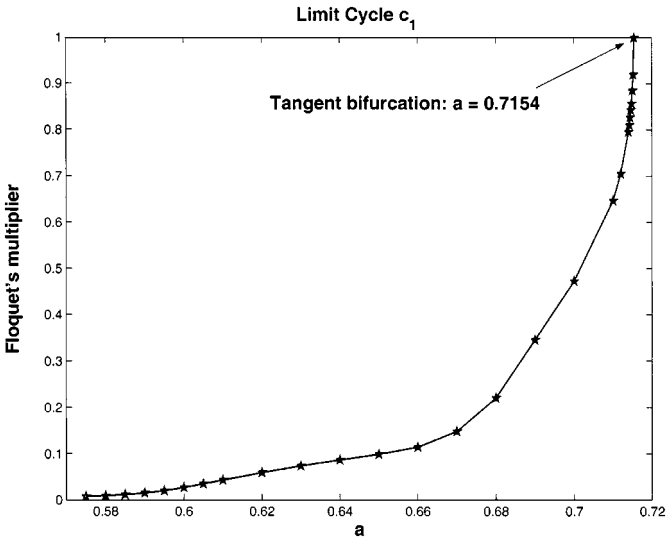

Fig. 5. Limit cycle c_1: most significant FM, versus a.

We have computed the Floquet's multipliers (FMs) of cycle c_1, by exploiting the algorithm reported in [17] [that requires to compute the first-order derivative of the output function $f_\varepsilon(\cdot)$]. Apart from the structural unitary FM, only one FM is significantly different from zero and therefore determines the limit cycle bifurcation: such a FM is reported in Fig. 5 as a function of a. It is seen that for $a = 0.7154$ this FM reaches the value 1, i.e., the limit cycle c_1 disappear through tangent bifurcation. The projection of the steady-state trajectory onto the plane (x_{11}, x_{12}) is shown in Fig. 6, for some values of the parameter a within the range of existence of c_1, i.e., $a \in [0.575, 0.7154]$. It is worth noting, that, according to the coordinate transformations (6) and (7), for $a \in [0.575, 0.7154]$, three other cycles coexists, i.e., $\mathcal{T}(c_1)$, $\mathcal{O}(c_1)$ and $\mathcal{O}[\mathcal{T}(c_1)]$. Such limit cycles present the same properties of c_1.

The simulation shows that for $a > 0.65$ another stable limit cycle emerges: such a cycle is denoted with c_2. The most significant FM

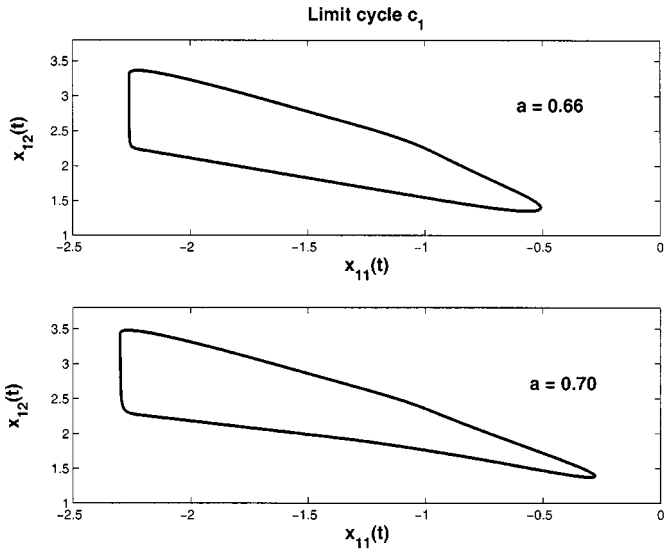

Fig. 6. Limit cycle c_1: projection of the trajectory onto the plane (x_{11}, x_{12}).

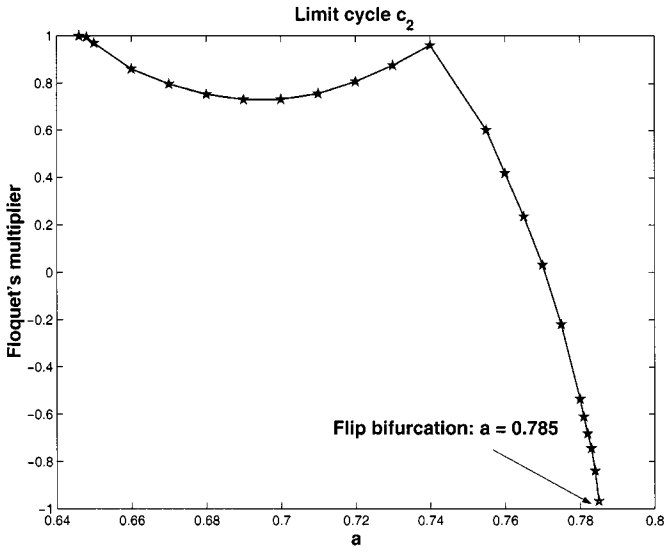

Fig. 7. Limit cycle c_2: most significant FM, versus a.

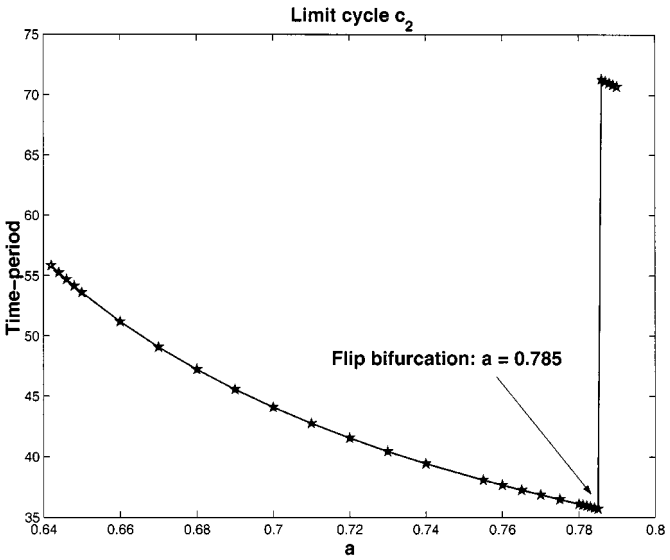

Fig. 8. Limit cycle c_2: time period versus a.

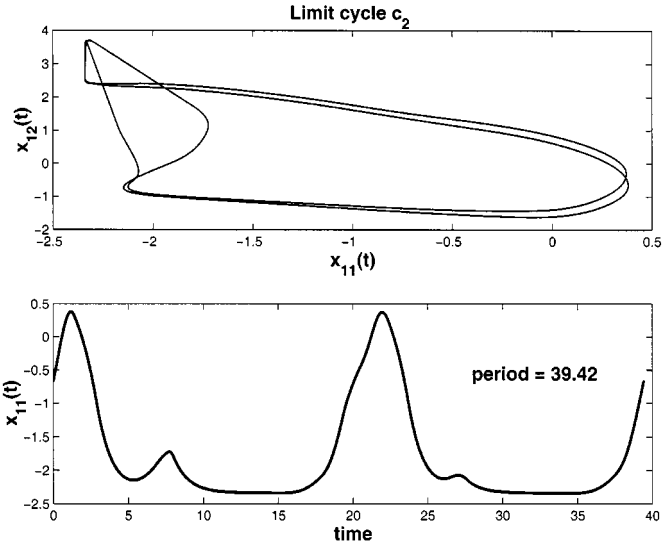

Fig. 9. Limit cycle c_2: projection of the trajectory onto the plane (x_{11}, x_{12}); steady-state waveforms of $x_{11}(t)$ for $a = 0.74$.

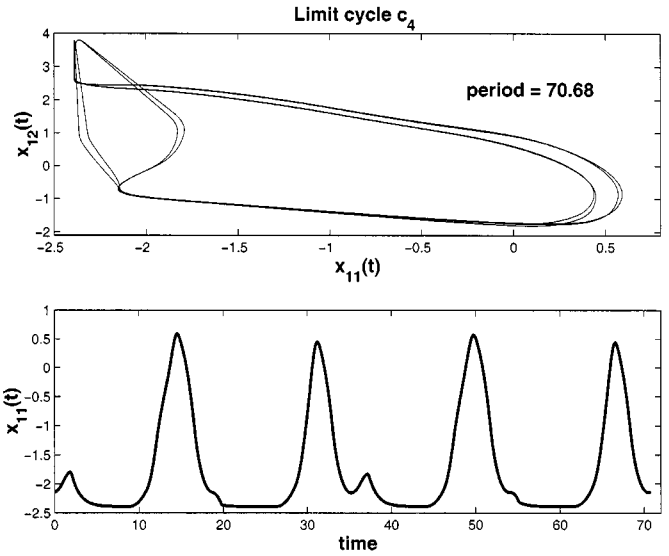

Fig. 10. Limit cycle c_4: projection of the trajectory onto the plane (x_{11}, x_{12}); steady-state waveforms of $x_{11}(t)$ for $a = 0.79$.

associated to c_2 is reported in Fig. 7, as a function of a. The analysis of the FMs shows that c_2 originates through a tangent bifurcation (as a approaches 0.65 from the right, one FM approaches 1); by increasing a, one FM approaches -1 and this reveals that c_2 undergoes a typical period doubling (flip) bifurcation, for $a = 0.785$. As a result of this bifurcation, c_2 becomes unstable and a new cycle (denoted with c_4) of period approximately twice arises (see Fig. 8). The main characteristics of these two cycles are reported in Figs. 9 and 10.

By further increasing a, a sequence of period doubling bifurcation leading to a chaotic attractor is observed (see Fig. 11, for $a = 0.8$). The Lyapunov exponents associated to the cycles c_2 (for $a = 0.74$) and to the chaotic attractor, obtained for $a = 0.8$, have been computed, by using the algorithm presented in [18, Ch. 3] and exploiting INSITE, the software tool described in [19]. The program output is reported in Table I. In both the cases (limit cycle c_2 and chaotic attractor), INSITE explicitly suggests that (according to the used internal tolerance) the Lyapunov exponent with the lowest absolute value be assumed zero. These results confirm the existence of a limit cycle (one zero Lyapunov

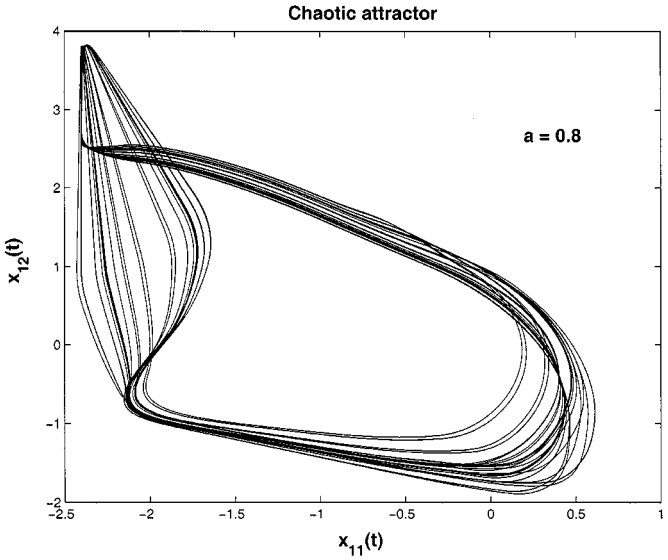

Fig. 11. Chaotic attractor, originated through the bifurcation of cycle c_2: projection of the trajectory onto the plane (x_{11}, x_{12}) for $a = 0.8$.

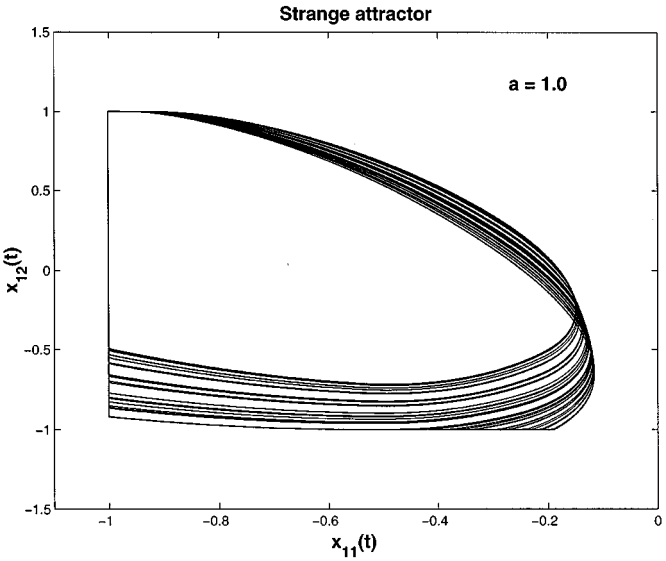

Fig. 12. Strange attractor in a CNN described by the modified VLSI model (8): projection of the trajectory onto the plane (x_{11}, x_{12}) for $a = 1.0$ and $b = 1.6$.

TABLE I
LYAPUNOV EXPONENTS FOR THE LIMIT CYCLE c_2 ($a = 0.74$) AND THE CHAOTIC ATTRACTOR, OBSERVED FOR $a = 0.8$

Lyapunov exponents	
Limit cycle c_2	Chaotic attractor
0.000833	0.036529
-0.016316	0.000034
-0.587443	-0.493471
-0.665539	-0.725800
-0.833612	-0.802559
-0.876804	-0.838617
-0.890424	- 0.869474
-0.931914	-0.919737
-0.989583	-0.995783

exponents) and of a chaotic attractor (one zero and one positive Lyapunov exponents).

We note that, by applying the coordinate transformations (6) and (7), in the range $a \in [0.575,\ 0.7154]$, it is easily proved the existence of three additional limit cycles i.e., $\mathcal{T}(c_1)$, $\mathcal{O}(c_1)$ and $\mathcal{O}[\mathcal{T}(c_1)]$. Similar arguments are valid for the limit cycles c_2 and c_4 and for the chaotic attractor: this means that for $a = 0.8$ four chaotic attractors coexists in the CNN state-space.

IV. MODIFIED CNN MODEL FOR VLSI IMPLEMENTATION

In this section we will show that a strange attractor, very similar to that of Fig. 11, also occurs for a CNN described by the modified model, reported in [15], that is more suitable for VLSI implementation.

In order to have a Lipschitz function, we describe the VLSI model [15], through the following state equations:

$$\dot{x}_{ij} = -x_{ij} - g(x_{ij}) + \sum_{|p|\le r,\,|q|\le r} A_{pq} x_{i+p,\,j+q} + \sum_{|p|\le r,\,|q|\le r} B_{pq} u_{i+p,\,j+q} + I \quad (8)$$

where the nonlinear function $g(\cdot)$ is defined as

$$g(x_{ij}) = \begin{cases} h(x_{ij}+1), & x_{ij} < -1 \\ 0, & |x_{ij}| \le 1 \\ h(x_{ij}-1), & x_{ij} > 1 \end{cases} \quad (9)$$

and h is assumed to be a positive real constant, large enough for approximating the nonlinear characteristic shown in [15, Fig. 4].

We consider a 3×3 network, described by the space-invariant template (5), with $b = 1.6$ and $h = 1000$. The simulation shows that the CNN exhibits a strange attractor, reported in Fig. 12, for $a = 1.0$. The strange attractor is rather similar to the chaotic attractor observed in the classical model (see Fig. 11) with the only difference that the trajectory is forced to remain into the unitary interval $]-1,\ 1[$. Note that chaos does not occur for the same value of a, because the two models (9) and (3) are described by a rather different set of parameters.

We have also verified that, due to the space-invariant structure, the existence of strange attractors does not depend on the number of cells $N \times M$, for both the Chua–Yang and the VLSI model.

V. CONCLUSIONS

We have investigated the occurrence of complex dynamic behaviors (i.e., bifurcation processes, strange and chaotic attractors) in first-order autonomous space-invariant CNNs. There are some reasons for carrying on this study: a) most CNN implementations exploits space-invariant templates; b) so far no example of complex dynamics has been shown in first-order autonomous space-invariant CNNs. Starting from a first-order autonomous CNN, described by a 2-D space-invariant template, we have investigated the equilibrium point bifurcation, leading to periodic attractors. Then, we have studied in detail the limit cycle bifurcation route to chaos, through the computation of the corresponding Floquet's multipliers and Lyapunov exponents.

We are confident that the identification of chaotic dynamics in such networks might open the possibility of developing, on the existing CNN chips, innovative chaos-based applications.

REFERENCES

[1] L. O. Chua and L. Yang, "Cellular neural networks: Theory," *IEEE Trans. Circuits Syst.*, vol. 35, pp. 1257–1272, Oct. 1988.

[2] ——, "Cellular neural networks: Applications," *IEEE Trans. Circuits Syst.*, vol. 35, pp. 1273–1290, OCt. 1988.
[3] L. O. Chua and T. Roska, "The CNN paradigm," *IEEE Trans. Circuits Syst. I*, vol. 40, pp. 147–156, Mar. 1993.
[4] "Special issue on bio-inspired processors and cellular neural networks for vision," *IEEE Trans. Circuits Syst. I*, vol. 46, Feb. 1999.
[5] *Special issue on spatio–temporal signal processing with analogic CNN visual microprocessors, J. VLSI Signal Processing*, vol. 23, no. 2/3, pp. 219–511, 1999.
[6] A. R. Vàzquez, M. Delgado-Restituto, E. Roca, G. Linan, R. Carmona, S. Espejo, and R. Dominguez-Castro, "CMOS Analogue Design Primitives," in *Toward the Visual Microprocessor—VLSI Design and Use of Cellular Network Universal Machines*, T. Roska and A. Rodriguez-Vazquez, Eds. Chichester, U.K.: Wiley, 2000, pp. 87–131.
[7] M. Salerno, F. Sargeni, and V. Bonaiuto, "A dedicated multi-chip programmable system for cellular neural networks," in *Analog Integrated Circuits and Signal Processing*. Norwell, MA: Kluwer, 1999, vol. 18, pp. 277–288.
[8] P. P. Civalleri and M. Gilli, "On stability of cellular neural networks," *J. VLSI Signal Processing*, vol. 23, pp. 429–435, 1999.
[9] F. Zou and J. A. Nossek, "Stability of cellular neural networks with opposite-sign templates," *IEEE Trans. Circuits Syst.*, vol. 38, pp. 675–677, June 1991.
[10] P. P. Civalleri and M. Gilli, "Global dynamic behavior of a three cell connected component detector CNN," *Int. J. Circuit Theory Applicat.*, vol. 23, no. 2, pp. 117–135, 1995.
[11] F. Zou and J. A. Nossek, "A chaotic attractor with cellular neural networks opposite-sign templates," *IEEE Trans. Circuits and Syst. I*, vol. 38, pp. 811–812, July 1991.
[12] ——, "Bifurcation and chaos in CNNs," *IEEE Trans. Circuits Syst. I*, vol. 40, pp. 166–173, Mar. 1993.
[13] M. Gilli, "Strange attractors in delayed cellular neural networks," *IEEE Trans. Circuits Syst. I*, vol. 40, pp. 849–853, Nov. 1993.
[14] G. Manganaro, P. Arena, and L. Fortuna, *Cellular Neural Networks: Chaos, Complexity and VLSI Processing*. New York: Springer-Verlag, 1999.
[15] G. Linan, R. Dominguez-Castro, S. Espejo, and A. R. Vàzquez, "Design of a large-complexity analog I/O CNNUC," in *Proc. ECCTD'99, Design Automation Day on Cellular Visual Microprocessor*, Stresa, Italy, Aug.–Sept. 1999, pp. 42–57.
[16] M. Gilli, M. Biey, P. P. Civalleri, and P. Checco, "Complex dynamics in cellular neural networks," in *Proc. ISCAS'01*, Sydney, Australia, May 2001.
[17] M. Farkas, *Perodic Motions*. New York: Springer-Verlag, 1994, pp. 58–59.
[18] T. S. Parker and L. O. Chua, *Practical Numerical Algorithms for Chaotic Systems*. New York: Springer-Verlag, 1989.
[19] ——, "INSITE—A software toolkit for the analysis of nonlinear dynamical systems," *Proc.EEE*, vol. 75, pp. 1081–1089, Aug. 1987.

Generalized State-Space Observers for Chaotic Synchronization and Secure Communication

M. Boutayeb, M. Darouach, and H. Rafaralahy

***Abstract*—In this brief, a simple and useful technique for both synchronization and secure communication of chaotic systems is developed. The proposed approach is based on generalized state space observer design for a class of nonlinear systems. By means of regular transformations we show that asymptotic stability is assured under mild conditions. To show accuracy and high performances of the proposed method, the well-known chaotic Lorentz system will be considered as an illustrative example.**

***Index Terms*—Chaotic systems, observer-based approach, secure communication, synchronization.**

I. Introduction

Synchronization in chaotic systems has received a large attention over the last decade. Since the pioneering work performed by Pecora *et al*. in [1], several synchronization schemes have been developed, see [8]–[10] just to mention few references. Observers based approach, in particular, becomes one of the attractive technique largely investigated in the recent research works [4], [6], [7], [12], [18]. Few results, however, have been established to deal with both synchronization and secure communication [2], [3], [5], [13]. The problem to deal with consists in injecting the information signal into the chaotic model and later, the received signal should be processed in order to construct the message. In [2], the authors use the Extended Kalman Filter based approach in communication where the information signal to be estimated is assumed to be slowly time varying. This assumption was also used in the recent work [3] based on standard identification methods and nice regular transformations of some well-known chaotic systems.

In [13], the authors used an unknown input observer scheme for synchronization and secure communication of linear discrete-time systems. Necessary and sufficient conditions for stability may be found in previous works [19], [20] (in a stochastic context, see [21]). We notice, however, that this approach can not be extended easily to nonlinear systems in particular when the information signals to be constructed are injected nonlinearly into the model.

For a class of nonlinear systems, a recent and attractive approach developed by Liao *et al.* in [5], is built upon two steps. The first one consists in computing the observer gain matrix for synchronization of a message free chaotic system. After, the information signal is added to the output signal and also injected linearly into the chaotic model through the observer gain matrix previously computed.

In this contribution, that may be seen as a generalization of the approach performed in [5], we investigate generalized nonlinear state space observers based approach for both chaos synchronization and secure communication. We introduce useful regular transformations to establish mild conditions for asymptotic convergence. Performances and easiness of implementation will be shown through the chaotic Lorentz system.

In order to make clear our contribution, let us point out the main differences with respect to the work of Liao *et al.* [5]. First, we consider chaotic systems with multiple outputs and multiple information signals

Manuscript received May 21, 2001; revised October 17, 2001. This paper was recommended by Associate Editor C. K. Tse.

The authors are with the University of Henri Poincaré, CRAN-CNRS, Cosnes et Romain 54400, France (e-mail: Mohamed.Boutayeb@iut-longwy.u-nancy.fr).

Publisher Item Identifier S 1057-7122(02)02268-7.